RESEARCH ARTICLE
Cytoskeleton, September 2010 67:586–598 (doi: 10.1002/cm.20469)

RNG1 is a Late Marker of the Apical Polar Ring in *Toxoplasma gondii*

Johnson Q. Tran,[1] Jessica C. de Leon,[1] Catherine Li,[1] My-Hang Huynh,[2] Wandy Beatty,[3] and Naomi S. Morrissette[1]*

[1]*Department of Molecular Biology and Biochemistry, University of California, Irvine, California 92697*
[2]*Department of Microbiology and Immunology, University of Michigan School of Medicine, Ann Arbor Michigan 48109*
[3]*Department of Molecular Microbiology, Washington University School of Medicine, St. Louis Missouri 63110*

Received 11 February 2010; Revised 3 June 2010; Accepted 24 July 2010
Monitoring Editor: George Bloom

The asexually proliferating stages of apicomplexan parasites cause acute symptoms of diseases such as malaria, cryptosporidiosis and toxoplasmosis. These stages are characterized by the presence of two independent microtubule organizing centers (MTOCs). Centrioles are found at the poles of the intranuclear spindle. The apical polar ring (APR), a MTOC unique to apicomplexans, organizes subpellicular microtubules which impose cell shape and apical polarity on these protozoa. Here we describe the characteristics of a novel protein that localizes to the APR of *Toxoplasma gondii* which we have named ring-1 (RNG1). There are related RNG1 proteins in *Neospora caninum* and *Sarcocystis neurona* but no obvious homologs in *Plasmodium* spp., *Cryptosporidium* spp. or *Babesia* spp. RNG1 is a small, low-complexity, detergent-insoluble protein that assembles at the APR very late in the process of daughter parasite replication. We were unable to knock-out the RNG1 gene, suggesting that its gene product is essential. Tagged RNG1 lines have also allowed us to visualize the APR during growth of *Toxoplasma* in the microtubule-disrupting drug oryzalin. Oryzalin inhibits nuclear division and cytokinesis although *Toxoplasma* growth continues, and similar to earlier observations of unchecked centriole duplication in oryzalin-treated parasites, the APR continues to duplicate during aberrant parasite growth. © 2010 Wiley-Liss, Inc.

Key Words: Apicomplexa, daughter buds, endodyogeny, MTOC, subpellicular microtubules

Introduction

The phylum Apicomplexa contains a number of pathogens which compromise human health or indirectly influence human well-being by infection of domesticated animals such as cattle and chickens [Levene, 1988]. *Toxoplasma gondii* is a human pathogen that causes serious opportunistic infections in immunocompromised individuals and can cause miscarriage or birth defects by infection of pregnant women [Black and Boothroyd, 2000]. *Toxoplasma* and other apicomplexans are obligate intracellular parasites that only grow and replicate within host cells. Parasite replication occurs after invasion of a host cell, within a membrane-bound vacuole, and continues until the host cell is lysed by the replicating parasites. Extracellular parasites released after lysis of host cells must rapidly invade new host cells in order to survive. Due to its size, relative ease of propagation in vitro and methods for molecular genetic manipulation, *Toxoplasma* also serves as a model system to study properties of the cytoskeleton shared by other apicomplexans [Dobrowolski and Sibley, 1997; Heintzelman and Schwartzman, 1997; Hettmann et al., 2000; Mann and Beckers, 2001; Herm-Gotz et al., 2002, 2006; Mann et al., 2002; Gaskins et al., 2004; Soldati and Meissner, 2004; Gilk et al., 2006; Gordon et al., 2008].

The proliferative (asexual) stages of apicomplexans cause the acute symptoms of disease. These stages contain two populations of microtubules: subpellicular microtubules, which give the parasite its crescent shape and spindle microtubules, which segregate chromosomes [Read et al., 1993; Hepler et al., 1966; Morrissette and Sibley, 2002a, 2002b]. These two populations of microtubules are nucleated from independent microtubule-organizing centers (MTOCs) [Russell and Burns, 1984; Nichols and Chiappino, 1987]. The apical polar ring (APR) is located at the parasite apex and nucleates subpellicular microtubules, while juxtanuclear centrioles are found at the spindle poles. Both the centriole and the APR MTOCs are unusual. Apicomplexan centrioles consist of two parallel cylinders composed of nine singlet microtubules and a central tubule [Morrissette and Sibley, 2002b]. These are distinct from conventional centrioles which are organized as two orthogonally organized cylinders composed of nine triplet microtubule blades. The APR is a circular MTOC only found in apicomplexan parasites [Russell and Burns, 1984]. Hook decoration demonstrates that

*Address correspondence to: Naomi S. Morrissette, Department of Molecular Biology and Biochemistry, University of California, Irvine CA 92697-3900. E-mail: nmorriss@uci.edu

Published online 24 July 2010 in Wiley Online Library (wileyonlinelibrary.com).

microtubules associated with the APR have their plus ends distal to the ring, as in all other established MTOCs. A species-specific fixed number of subpellicular microtubules (22 in *Toxoplasma*) laterally associate with the APR and extend towards the parasite posterior in close association with the cytosolic face of the parasite pellicle [Russell and Burns, 1984; Nichols and Chiappino, 1987]. The pellicle is a composite structure built by the association of the plasma membrane with an inner membrane complex (IMC) formed from flattened vesicles. While the plasma membrane surrounds the entire parasite circumference, the IMC terminates at the APR so that the extreme apex (where apical secretion occurs) is only enclosed by a single unit membrane.

The subset of apicomplexan parasites known as the Coccidia includes *Toxoplasma*, *Eimeria* spp., *Sarcocystis* spp., and *Neospora caninum*. Coccidians have a particularly complex apical cytoskeleton relative to other apicomplexans because they have an additional structure, the conoid, built from comma-shaped tubulin sheets which are organized into spiraling filaments that form a cone-shaped structure [Nichols and Chiappino, 1987; Morrissette et al., 1997; Hu et al., 2002b]. Additionally, above the conoid are two preconoidal rings. The conoid and the preconoidal rings can extend beyond the APR or retract within it to be surrounded by the basket of subpellicular microtubules. Conoid extension and retraction is a visible process during invasion and is dependent upon intact calcium signaling [Mondragon and Frixione, 1996; Pezzella et al., 1997; Monteiro et al., 2001; Del Carmen et al., 2009]. Conoid extension can be triggered in extracellular parasites by ionomycin treatment. When a *Toxoplasma* apical cytoskeleton fraction that includes the APR and conoid was analyzed by mass spectroscopy, proteomic data suggests that these structures do not contain conventional MTOC components [Hu et al., 2006]. However, replicating parasites must coordinate centriole duplication and nuclear division with production of APR associated with daughter parasites. Nascent daughter buds appear in close proximity to centrioles, and although there is not direct evidence for it, centrioles may regulate the timing and number of daughter APR structures.

Toxoplasma replicates by endodyogeny, a process of internal budding where daughter parasites are formed synchronously with nuclear division within the mother parasite [Radke et al., 2001; Hu et al., 2002a; Morrissette and Sibley, 2002b; Stedman et al., 2003; Gordon et al., 2008; Nishi et al., 2008]. During replication, the nuclear membrane remains intact and spindle microtubules form an intranuclear spindle to coordinate chromosome segregation. Unlike the linear organization of most spindles, *Toxoplasma* spindle microtubules are inserted into the nucleus at an acute angle that persists during chromosome segregation [Striepen et al., 2000; Morrissette and Sibley, 2002b; Swedlow et al., 2002]. Spindle poles are associated with cytoplasmic centrioles, and spindle microtubules pass through an electron-dense invagination of the nuclear membrane (the centrocone) to coordinate mitosis. Centrioles and the Golgi apparatus are adjacent to the apical end of the nucleus in interphase parasites. Early in the replication process centrioles migrate to the basal end of the nucleus, duplicate, then return to the apical end of the nucleus where they localize to opposite ends of the single Golgi stack, which divides into two [Pelletier et al. 2002; Hartmann et al., 2006; Nishi et al., 2008]. Early in parasite replication, the TgMORN1 protein localizes to duplicated centrocone structures and labels adjacent rings which encircle the duplicated centrioles and mark initiation of two daughter cell buds [Gubbels et al., 2006; Ferguson et al., 2008; Hu, 2008]. Daughter buds consist of IMC and associated subpellicular microtubules nucleated from daughter APR structures. As these buds grow, TgMORN1 moves with the growing end of the parasite posterior in association with other proteins termed the basal complex. Each daughter bud contains secretory organelles (rhoptries and micronemes) that are essential for host cell invasion and unique to the Apicomplexa [Hu et al., 2002a; Hu, 2008; Nishi et al., 2008]. The Golgi apparatus, centrioles, an essential plastid termed the apicoplast and chromosomes segregate as the ends of the horseshoe-shaped dividing nucleus are pulled into the daughter buds. Centrioles are found in close proximity to the spindle poles and the location of the nascent APR [Striepen et al., 2000; Morrissette and Sibley, 2002b; Hu, 2008]. The spatial and temporal association of the centrioles with forming APR suggests that centrioles may regulate APR biogenesis during replication by endodyogeny.

Intracellular *Toxoplasma* fail to form daughter parasites when their microtubules are disrupted by oryzalin, a protozoan-specific microtubule disrupting compound that does not affect host cell microtubules [Stokkermans et al., 1996; Shaw et al., 2000; Morrissette and Sibley, 2002b]. These parasites cannot undergo mitosis or cytokinesis, but maintain metabolic activity with continued protein synthesis and DNA replication. If oryzalin is washed away after 24–48 hours, subpellicular microtubules are nucleated and form daughter parasites [Morrissette and Sibley, 2002b]. However, since the polyploid nucleus cannot be correctly segregated into individual genomes, daughter parasites lack nuclei or have incomplete genome complements that are lethal. Parasites under oryzalin treatment continue to duplicate their centrioles as assessed by centrin staining [Shaw et al., 2000; Morrissette and Sibley, 2002b].

The unusual properties of microtubules and MTOCs in apicomplexan parasites suggest that these elements may represent excellent targets for therapeutic agents. In particular, the unique organization and constituents of the APR would ensure that antiparasitic drugs that act on these components would not have host toxicity due to the presence of parallel human structures. In this study we describe a novel marker of the APR in *Toxoplasma*. We have named this MTOC component RNG1 and report its properties and behavior in replicating tachyzoites. RNG1 is the first protein component of the APR to be described; it will provide a useful marker for characterizing APR biogenesis during parasite replication and for defining additional molecular components that build

this novel MTOC. In this study we have used RNG1 as a marker to discover that like centrioles, the APR continues to duplicate in parasites when mitosis and cytokinesis are inhibited by microtubule disruption.

Materials and Methods

Culture of Host Cells and Parasites

Toxoplasma lines were grown in human foreskin fibroblast (HFF) host cells as previously described [Roos et al., 1994]. Specific transgene and knock-out selection conditions are described below, as is treatment with the parasite microtubule-disrupting compound oryzalin.

Tagging the Endogenous 49.m03355 (RNG1) Gene

Creation of the stable parasite line with a fusion of 49.m03355 to YFP was previously described [Huynh and Carruthers, 2009]. To tag the endogenous copy of 49.m03355 with mCherry, a 2.169 kB fragment terminating with the end of the predicted open reading frame was amplified from the *Toxoplasma* genome (RH strain) with primers (5′-TACTTCCAATCCAATTTAATGCGACATGCTGTCC AGTAGC-3′ and 5′-TCCTCCACTTCCAATTTTAGCCGC CAGGTAGTAGACAGG-3′). This was cloned into the pmCherry.LIC.DHFR vector to create an in-frame fusion to the mCherry fluorescent protein. This plasmid was integrated into the endogenous locus in a *Ku*80 knock-out line using established methods [Huynh and Carruthers, 2009]. Stable RNG1-mCherry transgenic lines were created by selection in 1 μM pyrimethamine and single-cell cloning.

Conceptual Translation and Protein Alignment

The predicted amino acid sequence of 49.m03355 was used to search for related proteins encoded by apicomplexan expressed sequence tags (ESTs). A number of sequences (NcEST3d98f07.y1, NcEST3d67f09.y1, NcEST3d50d10.y1, NcESTqab58c03.y1, NcESTqab50d03.y1, NcEST3d31f02.y1, NcEST3d32f09.y2, NcEST3c95b01.y3, NcEST3c41c05.y1, NcEST3d91h09.y1, NcEST3d58e02.y1, NcEST3d83c06.y1, NcEST3d79d04.y1 and NcEST3d47g06.y1) from the closely related coccidian *Neospora caninum* were identified as highly related using BlastX [Gish and States, 1993; States and Gish, 1994] of the non-human, non-mouse EST collection at NCBI. These sequences were assembled using Sequencher (GeneCodes). The "work in progress" *Sarcocystis neurona* genome (at ~7-fold coverage) was queried using tBLASTn with the *Toxoplasma* RNG1 protein sequence. Access to the *Sarcocystis* data was kindly provided by Daniel Howe and Christopher Schardl at the Advanced Genetic Technologies Center of the University of Kentucky. The predicted amino acid sequence of the *Neospora* and *Sarcocystis* RNG1 homologs was aligned with the *Toxoplasma* protein using ClustalW2 (www.ebi.ac.uk) [Higgins et al., 1996].

Immunofluorescence Labeling and Fluorescence Microscopy

HFF cells on 12 mm circular glass coverslips were infected with RNG1-YFP or RNG1-mCherry expressing parasites. Intracellular parasites were fixed, permeabilized, and stained as previously described [Morrissette and Sibley, 2002b]. Antibodies used to stain parasites include mouse monoclonal antibodies against GFP (Roche), ISP1 (gift of Peter Bradley), [Beck et al., in press], centrin (20H5, kind gift of Jeff Salisbury), anti-P30/SAG1 (DG52) [Burg et al., 1988] and a *Toxoplasma*-specific tubulin sera made in rabbit [Morrissette and Sibley, 2002b]. These antibodies were detected with Alexa-594 and 488 conjugated antibodies (Invitrogen). DNA was visualized by DAPI staining and samples were mounted in a polyvinyl alcohol-based mounting medium. Images were collected on a Zeiss Axiovert 200M using the Axiovision camera and software and exported for manipulation in Photoshop 8.0.

Detergent Extraction for Immunoblots and Immunofluorescence

Freshly lysed parasites were purified from host cell debris by filtration through 3.0 μm polycarbonate filters (GE Water & Process Technologies) and collected by centrifugation at 1000g for 20 minutes at 4°C. These samples were suspended in PBS containing 1% Triton X-100 (Fisher Scientific) and incubated at RT for 10 minutes. Improved resolution of RNG1-YFP association with subpellicular microtubules was achieved by extracting isolated RNG1-YFP parasites with 10 mg/mL deoxycholate (DOC) in PBS for 25 minutes at RT. Detergent-extracted parasite samples for immunofluorescence were settled onto poly-L-lysine (Sigma) coated coverslips for 15 minutes at RT. These samples were fixed with 10% formalin solution (Sigma) or −20°C acetone (Fisher Scientific) prior to processing for immunofluorescence (see above). Samples for immunoblot analysis were spun at 3750 RPM to separate insoluble and soluble material. The soluble fraction was TCA precipitated and both soluble and insoluble fractions were suspended in Tris Tricine SDS Sample Buffer (NuSep) for resolution on a 4–20% gradient Tris-HCl polyacrylamide gel (Biorad). After transfer to nitrocellulose (Whatman) and blocking in 5% non-fat milk at 4°C overnight, the blots were probed with an anti-GFP antibody (Roche) and Alexa 488 anti-mouse secondary antibody (Invitrogen) and resolved with a Typhoon Trio Variable Mode Imager (GE Healthcare).

Conoid Extrusion

Freshly lysed out tachyzoites were purified from host cell debris by filtration through 3 μm polycarbonate filters and collected by centrifugation at 70 *g* for 5 minutes at 4°C. These samples were washed in HEPES-buffered saline and suspended in HEPES-buffered saline containing 5 μM ionomycin (Sigma) and 5 mM $CaCl_2$ (Sigma) and incubated at RT for 5 minutes [Mondragon and Frixione, 1996; Pezzella

et al., 1997; Monteiro et al., 2001]. Samples were then fixed for 10 minutes in 1% glutaraldehyde in PBS prior to microscopy.

Electron Microscopy

Epon-embedded parasite samples for electron microscopy were generated using the Tilney "double fix" as described previously [Morrissette and Sibley, 2002b].

Immunogold Localization

Freshly lysed tachyzoites from the stable RNG1-YFP line were isolated by filtration and centrifugation as described above. Parasites were fixed in 4% paraformaldehyde and 0.01% glutaraldehyde in 100 mM PIPES for 1 hour at 4°C. Samples were embedded in 10% gelatin and infiltrated overnight with 2.3M sucrose with 20% polyvinylpyrrolidone in PIPES at 4°C. After samples were frozen in liquid nitrogen and sectioned with a cryo-ultramicrotome, sections were probed with an anti-GFP antibody (Abcam). Antibody binding was detected with 18-nm colloidal gold-conjugated anti-rabbit antibody (Jackson), stained with uranyl acetate/methylcellulose, and analyzed by electron microscopy.

Oryzalin Treatment

Nearly confluent HFF host cells on 12 mm circular glass coverslips were infected with RNG1-YFP tachyzoites and grown in media with 2.5 μM oryzalin. After 24 hours, coverslips were harvested for immunofluorescence. Immunofluorescent staining was used to follow the localization of centrin, tubulin, RNG1-YFP and DNA.

RNG1 Gene Knock-Out

We attempted to disrupt the RNG1 gene with a RNG1 knock-out construct intended to replace the RNG1 (49.m03355) locus with the hypoxanthine-xanthine-guanine phophoribosyltransferase (HPT) gene. The RNG1 knock-out construct is based on the pMini-GFP.hh knock-out vector [Karasov et al., 2005; Gilbert et al., 2007]. The pMini-GFP.hh consists of the HPT gene for drug selection and a downstream GFP that differentiates heterologous recombination events. The RNG1 5′ flank insert (5050 bp) was amplified from RH strain genomic DNA with primers 5′-GCGGGCCCGACCGCTTGGAAGTTCGAGGC-3′ and 5′-GCGGGCCCTCGTCGTGGAAGAACAAAGGATCC-3′. The RNG1 3′ flank insert (4426 bp) was amplified with primers 5′-GCACTAGTATCATGTCGGCGTGATTTTCG-3′ and 5′-GCACTAGTGTCATTTAGAAAGAACGCAG GAGG-3′. The 5′ flank insert was cloned into the *Apa*I site upstream of the HPT gene. The 3′ flank insert was cloned into the *Spe*I site downstream of the HPT gene. The completed RNG1 knock-out construct (pKO-RNG1) was linearized overnight with *Not*I. A standard transfection protocol was used to electroporate 30 μg of DNA into both RHΔhpt and RHΔ*ku*80Δhpt parasite lines. Transfected parasites were selected with media supplemented with both mycophenolic acid and xanthine at 50 μg/ml. Clonal populations of stable parasite lines were generated by limiting dilution. Clones were screened by fluorescence microscopy and both GFP positive and negative lines were probed for gene deletion by amplification of a 5′-genome region with primers CTGTAGCGACAGAGTTTGGCGGATTTGC and GAC GTGGTCGAAGTCGCGGAACATCTCG and amplification of a 3′-genome region with primers TGGCGTCC AAACCCATTGAAGACTACG and CGGACTGAGAGTTC CAGAGGATCAAGTGC.

Ectopic Expression of the RNG1 Protein

A RNG1-YFP vector driven by the strong α1-tubulin promoter was generated by modifying the GRASP55-YFP construct [Hartmann et al., 2006] which contains the selectable marker chloramphenicol. The GRASP55 gene was replaced by the RNG1 coding sequence in frame with YFP and transfected into RH strain parasites. Lines that stably express this construct were selected in 20 μM chloramphenicol.

Induced RNG1 Degradation

We generated constructs to introduce the human FKBP12 destabilization domain (ddFKBP) at the amino or carboxy-termini of our established RNG1-YFP construct (with a DHFR selectable marker) [Herm-Gotz et al., 2007]. The carboxy-terminal construct was generated by removing the stop codon following YFP and inserting the ddFKBP coding sequence and a stop codon to follow the YFP sequence. The amino terminal construct was generated by inserting the ddFKBP domain upstream of the RNG1-YFP coding sequence in the LIC vector. Since the RNG1 coding sequence is so small, there is an additional 1.93 kB upstream of the amino terminal ddFKBP domain in our modified vector. These plasmids were integrated into a *Ku*80 knock-out line by selection in 1 μM pyrimethamine and single-cell cloning of resistant transformants. We validated that the FKBP constructs were correctly integrated into lines that showed RNG1-YFP labeling using primers TCGCAATT GATGGGAGTGCAGGTGGAAAC and TGCCGCCAGG TAGTAGACAGGTGGAGG for the ddFKBP-RNG1-YFP construct and primers ATCGCGCTAATTCCCTCGCCGG and TCGCAATTGTTCCGGTTTTAGAAGCTCCAC for the RNG1-YFP-ddFKBP construct.

Results

Toxoplasma, *Neospora,* and *Sarcocystis* Encode a Conserved Small Protein

The hypothetical gene 49.m03355 annotated by the *Toxoplasma* genome project encodes a small protein which lacks conservation with any previously characterized proteins. Abundant ESTs corresponding to mRNA for this protein as well as mass spectroscopy hits in two preparations of detergent-insoluble proteins from *Toxoplasma* (ToxoDB.org: the Hu and Wastling projects) indicate that this postulated gene

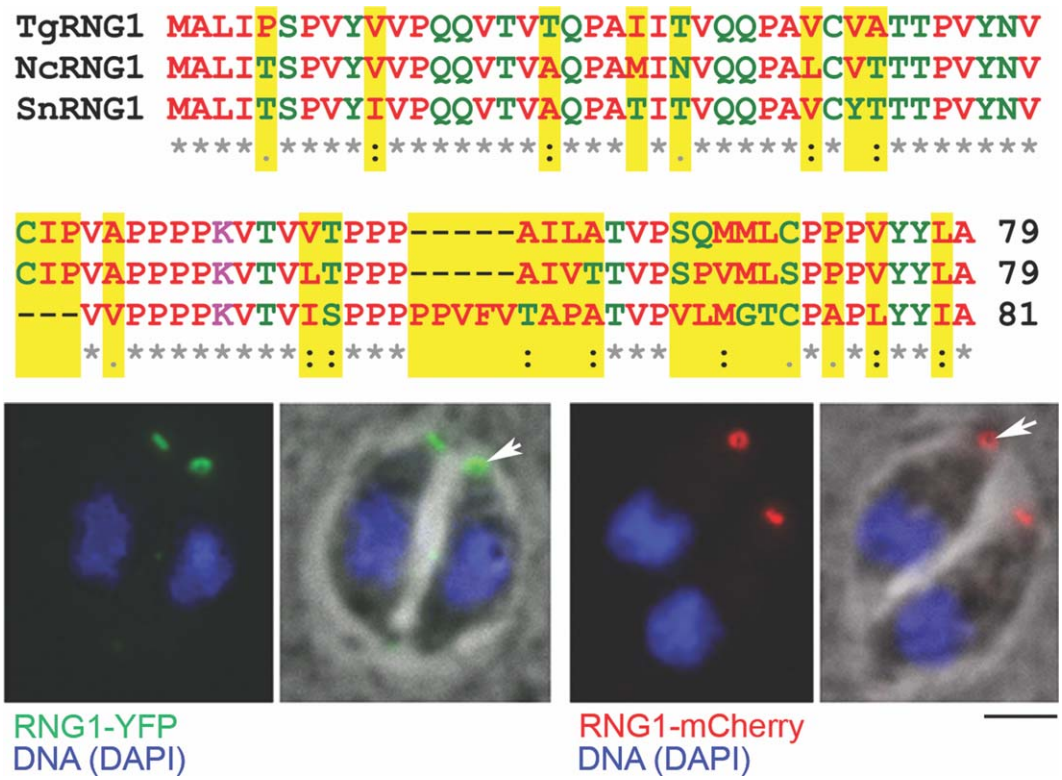

Fig. 1. The *Toxoplasma* 49.m03355 gene encodes a small, low complexity protein that localizes to an apical ring. (Top) Clustal alignment of the amino acid sequences of *Toxoplasma* 49.m03355 (TgRNG1), *Neospora* (NcRNG1), and *Sarcocystis* (SnRNG1) homologs. These low complexity proteins are nearly 25% proline. Note that the *Sarcocystis* homolog has a three residue deletion, a five residue insertion and sequence divergence in regions of the protein that are of higher complexity (i.e. not polyproline stretches). (Bottom, left) A *Toxoplasma* line with a stable fusion of the endogenous 49.m03355 (RNG1) gene to YFP (green) has a small fluorescent apical ring. (Bottom, right) Tachyzoites expressing a stable fusion of the endogenous 49.m03355 (RNG1) gene to mCherry (red) also show apical ring localization. DNA stained with DAPI is blue. Scale bar = 2 μm.

is likely to encode a protein that is expressed in *Toxoplasma* tachyzoites [Cohen et al., 2002; Hu et al., 2006]. Moreover, conceptual translation of similar EST sequences from the closely related parasite *Neospora caninum* indicates that it has a related protein (Fig. 1, top). The protein predicted by the *Toxoplasma* genome project annotation has two possible in-frame start sites. The *Neospora* protein lacks any homology to the region after the first predicted start site, strongly suggesting that the protein begins with the second methionine. This 79 amino acid protein is overwhelmingly composed of non-polar amino acids (54 or 68%), has a single basic lysine, 24 uncharged polar residues (30%) and lacks any acidic residues. The protein is dominated by prolines (18 or 23%); these features suggest that it could be a peripherally associated membrane protein.

We also searched genome projects for the coccidian parasite species *Sarcocystis neurona* and *Eimeria tenella*. *S. neurona* has a conserved homolog, but *E. tenella* does not have an unambiguously related protein. The *Sarcocystis* protein is two amino acids longer than the *Toxoplasma* or *Neospora* proteins and has a three amino acid deletion as well as a five amino acid insertion (Fig. 1, top). Amino acid substitutions to this small protein in closely related species as well as its low overall complexity make it difficult to identify homologs in other apicomplexans. The exact protein does not appear to be represented in the genomes of *Plasmodium* spp. and *Cryptosporidium* spp.; however, there are several proline-rich proteins in these organisms which may represent the orthologous protein.

In-Frame Fluorescent Protein Fusions to 49.m03355 Label the Apical Polar Ring

Since independent stable lines that express a carboxy terminal fusion of the 49.m03355 protein to either YFP [Huynh and Carruthers, 2009] or mCherry display a fluorescent ring at the apex of *Toxoplasma* tachyzoites, we have named the 49.m03355 protein RNG1 (Fig. 1, bottom). Labeling with a *Toxoplasma*-specific tubulin antibody illustrates that the subpellicular microtubules originate in the region of the ring (Fig. 2a). During replication by endodyogeny, daughter parasites visualized with an anti-tubulin protein do not display RNG1 labeling at the APR until nuclear division is complete (Figs. 2b and 2c). Mature daughter parasites integrate RNG1-YFP into the APR prior to emerging from the mother parasite. The residual body discarded after completion of replication contains both the maternal microtubules and APR as labeled by RNG1 (Fig. 2d). We have previously observed discarded maternal subpellicular microtubules in the residual body of replicating tachyzoites

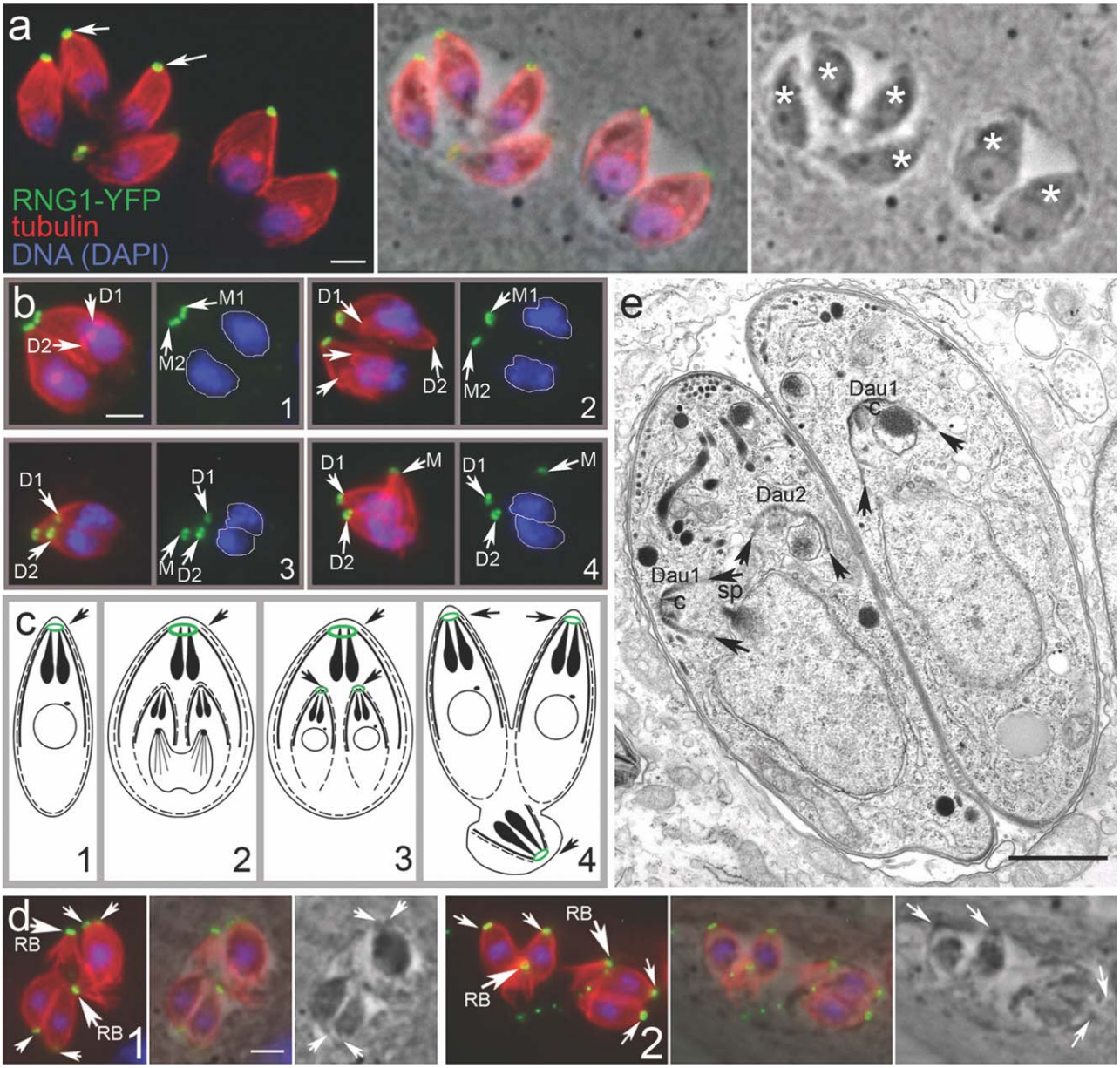

Fig. 2. RNG1 is a late marker of *Toxoplasma* apical polar ring. (a, left) *Toxoplasma* tachyzoites within two adjacent parasitophorous vacuoles are enclosed in a basket of subpellicular microtubules (red). These microtubules originate in the apical region proximal to the location of RNG1-YFP (green). (a, middle) Merged fluorescence and phase-contrast images and (a, right) phase-contrast image are also shown with the individual parasites indicated with asterisks. Scale bar = 2 μm. [(**b**), Images 1–4] Immunofluorescence of tubulin (red) and RNG1-YFP (anti-GFP, green) with DNA in blue (DAPI) in tachyzoites at the replication stages illustrated in (**c**). M = mother parasite, D = daughter parasite. Scale bar = 2 μm. (**c**) A schematic of *Toxoplasma* replication by endodyogeny to illustrate the late appearance of RNG1-YFP in daughter parasites. Although daughter buds are built before nuclear division is complete (2), RNG1-YFP only appears on daughter buds after nuclear scission (3). As the daughter parasites adopt the maternal plasma membrane, maternal microtubules and RNG1-YFP are discarded in the residual body (4). (**d**) The high frequency of emerging daughter parasites (arrows) which are captured in the process of discarding maternal microtubules and APR into a residual body (arrows, RB) suggests that this process is an established element of parasite replication. Two examples of emerging daughter parasites are illustrated with fluorescence, merged phase-contrast and fluorescence and phase-contrast alone images. Scale bar = 2 μm. (**e**) Electron microscopy of two replicating parasites: the left-most parasite has two daughter buds (Dau) visible as well as half of the spindle (sp) while the parasite on the right has only one of two daughter buds visible in the section. Arrows indicate nascent daughter buds, which contain intact conoids (c) and IMC with associated subpellicular microtubules (visible as hatches on the daughter 2 IMC). Since microtubules associated with daughter buds are present before nuclear scission is complete, microtubule nucleation occurs before RNG1 association with the APR, which occurs after nuclear scission. Scale bar = 1 μm.

[Morrissette and Sibley, 2002b). Although it is simple to visualize daughters emerging from mother parasite remnants with RNG1 and tubulin labeling, we do not think that YFP tagging increases the stability of this structure. It is more likely that fluorescent tagging of microtubules and the APR makes it easier to identify structures that are

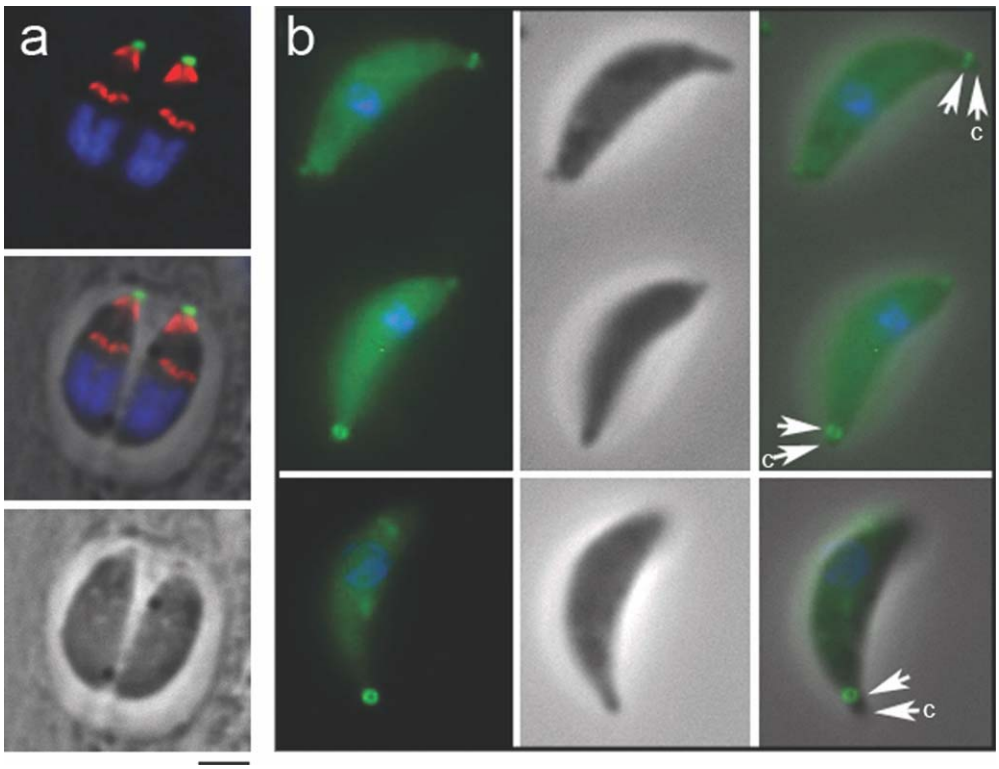

Fig. 3. RNG1 is localized above the inner membrane complex and beneath the extended conoid. (a) Labeling of the ISP1 protein (red) and RNG1-YFP (green) illustrates that these proteins have apical but non-overlapping localization patterns, where RNG1 surmounts the ISP1 cap in mother parasites. In forming daughter buds, ISP1 is assembled before RNG1. DNA distributed in horseshoe shaped nuclei is labeled with DAPI (blue). Scale bar = 2 μm. (b) Ionomycin-mediated conoid extrusion in extracellular parasites illustrates that RNG1 lies below the tip of the extended conoid (arrow) and is therefore not a pre-conoidal ring component. Images are (left to right) fluorescence, phase-contrast, and merged fluorescence and phase-contrast.

difficult to observe by either phase-contrast or electron microscopy.

RNG1 Localizes Beneath the Extended Conoid and is a Late Component of Replicating Parasites

Labeling with an antibody to the IMC sub-compartment protein ISP1 shows that RNG1 staining is anterior to ISP1, a component of the apical membrane cap region of the IMC [Beck et al., in press] (Fig. 3a). Moreover, as described above, RNG1 is not found on developing daughter parasites, which can be seen by segregation of the horseshoe-shaped nuclei into two daughter buds which each show apical cap labeling with the ISP1 antibody. When freshly-lysed extracellular tachyzoites are treated with 5 μM ionomycin to stimulate conoid extension, RNG1 is localized beneath the extruded conoid (Fig. 3b), indicating that it is a component of the APR rather than the two pre-conoidal rings which surmount the conoid [Nichols and Chiappino, 1987]. Electron microscopy of immunogold labeled sections reveals that YFP-tagged RNG1 is localized at a discrete region of the apex, internal to the IMC (Fig. 4a). In images where the conoid is extended, label is found beneath the conoid (Figs. 4b and 4c) and in some cases, coincides with the region where the IMC terminates at the APR (see arrow, Fig. 4c). In parasites where the conoid is retracted beneath the APR, gold label localizes between the conoid filaments and the IMC (Figs. 4d–4f). Glancing sections that reveal the electron-dense APR show labeling around its circumference (Fig. 4g).

RNG1 is a Detergent-Insoluble Component of the Mature Apical Polar Ring

Detergent extraction of YFP-tagged RNG1 parasites indicates that the protein is insoluble, a hallmark of many *Toxoplasma* cytoskeletal proteins. When extracellular tachyzoites are extracted with 1% Triton X-100, the RNG1 protein remains with the detergent-insoluble membrane skeleton (Fig. 5a). As a control for extraction, anti-P30 antibody shows that the GPI-linked surface protein SAG1 is absent from extracted parasites. Immunoblots probed with anti-GFP antibody show that RNG1-YFP appears as a single band at ~36 kDa, consistent with its predicted molecular weight (Fig. 5b). This RNG1-YFP band is present in whole-cell lysates, is retained in the detergent-insoluble fraction but is largely absent from the detergent-soluble fraction and completely missing in untransfected RH strain parasites. When extracellular RNG1-YFP parasites are extracted in 10 mg/mL deoxycholate, their subpellicular microtubules, APR and conoid are freed from other parasite components (Figs. 5c and 5d). The free but stable subpellicular microtubules can be visualized

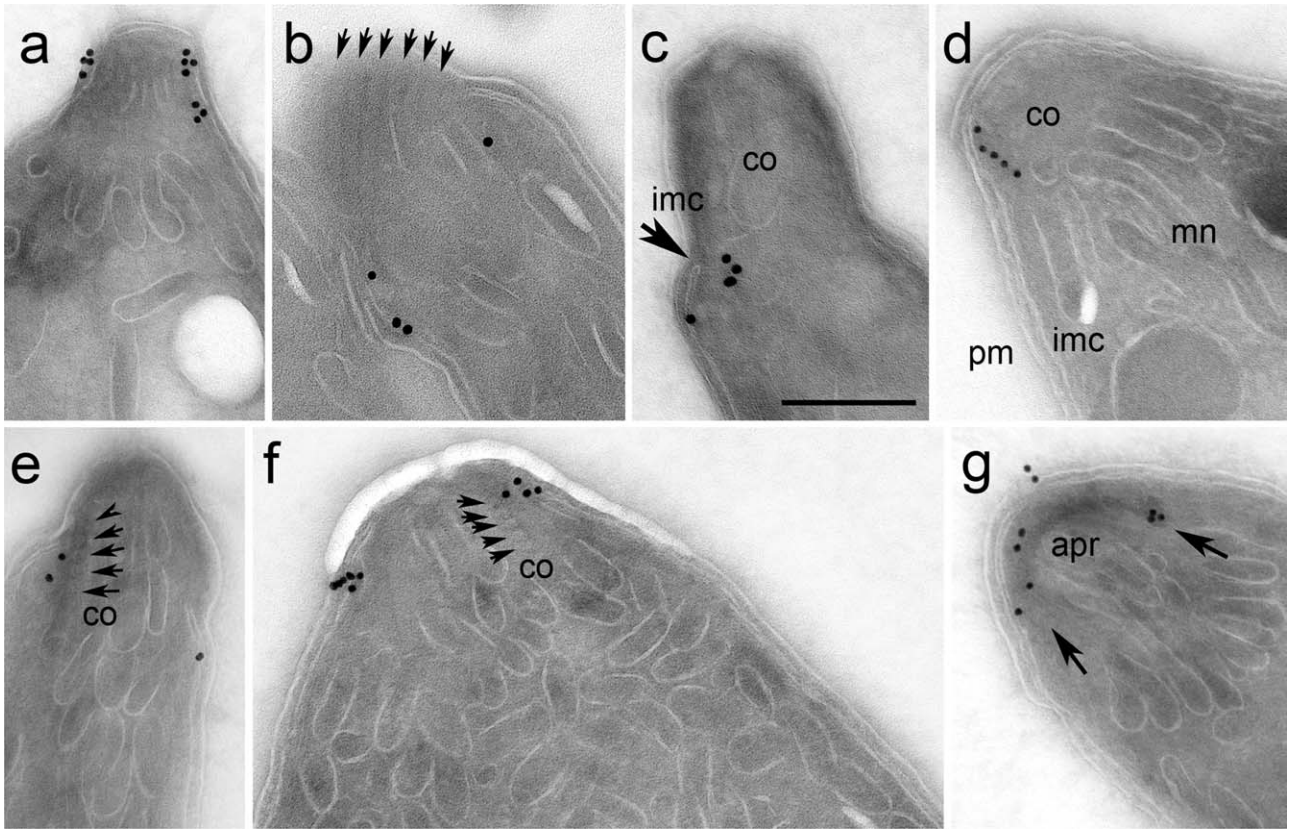

Fig. 4. Immunogold labeling of YFP-tagged RNG1 with electron microscopy illustrates that RNG1 is found in the apical region of *Toxoplasma* tachyzoites (a–g). (a) Gold labeling is located in a discrete region of the cytosolic face of the parasite pellicle in the apical region. The label lies beneath the extended conoids (co) whether the section is grazing so that conoid filaments are visible (arrows, b) or through the conoid, such that the terminal portion of the IMC is visible (arrow, c). Panel d illustrates that gold is restricted to the region adjacent to the conoid (co), above the micronemes (mn) and interior to the plasma membrane (pm) and inner membrane complex (imc). In samples where sections bisect individual conoid filaments (arrows, e and f), RNG1 labeling is between the base of the conoid and the IMC. In a grazing section of the APR, this structure appears as a dark semicircle (g, arrows) and shows labeling along its entire length. Scale bar in panel c = 200 nm.

extending from the circular RNG1-YFP tagged APR structure (Fig. 5c, Images 1–4). When parasites are viewed with the APR edge-on (Fig. 5c, Images 5 and 6), it is clear that there is a gap between tubulin staining of the extended conoid above the APR and tubulin staining of the subpellicular microtubules below the RNG1-YFP. The sample shown in Fig. 5c (Image 7) has a retracted conoid or has lost the conoid structure but retains the RNG1-YFP labeled APR. In some samples, extraction and manipulation causes APR fragmentation. In these cases, RNG1-YFP is located at the minus end tips of the subpellicular microtubules (Fig. 5d).

RNG1 is Likely to be Essential for Parasite Survival

We attempted to eliminate the RNG1 protein using both gene deletion and targeted protein degradation techniques. We were not able to eliminate the RNG1 protein suggesting that it is essential for parasite survival. First, we tried to delete the RNG1 gene using a targeting construct containing the hypoxanthine-xanthine-guanine phophoribosyltransferase (HPT) gene [Karasov et al., 2005; Gilbert et al., 2007]. In cases of non-homologous integration of this vector, the parasites express GFP. In five independent experiments using RHΔ*ku*80Δhpt tachyzoites (Huynh and Carruthers, unpublished) and in five independent experiments using RHΔhpt, we were unable to identify parasites that had the knock-out construct inserted into the gene (data not shown). As an alternative strategy, we modified the LIC-YFP vector [Huynh and Carruthers, 2009] to create a carboxy terminal YFP fusion to the modified FK506 binding destabilization domain (ddFKBP) [Herm-Gotz et al., 2007]. Although we were able to create stable lines containing a carboxy-terminal ddFKBP domain, these lines did not show an appreciable decrease in RNG1-YFP in the absence of Shield1 (not shown). Since RNG1 is encoded by a small gene, we were also able to use a LIC vector containing the entire coding region and 1.93 kB upstream sequence to generate a construct where RNG1 was flanked by an amino-terminal ddFKBP domain and a carboxy-terminal YFP. When this construct was introduced into *Ku*80 null parasites, we were unable to induce ddFKBP-RNG1-YFP protein degradation by removal of the Shield1 ligand (Figs. 6a–e). One possibility is that rapid integration of RNG1 into the APR prevents

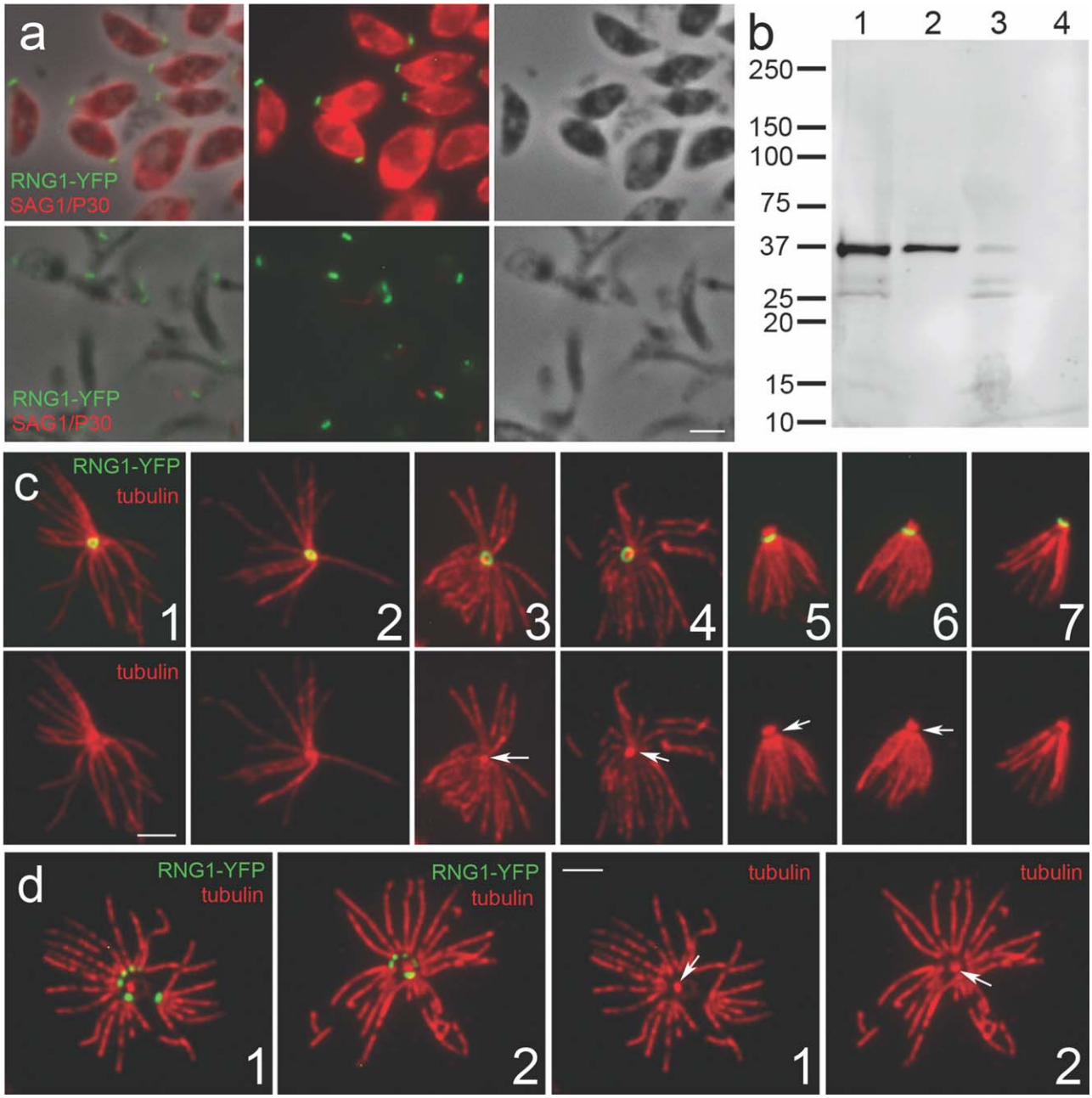

Fig. 5. RNG1 is a detergent-insoluble component of the *Toxoplasma* cytoskeleton. (**a**) Immunofluorescent labeling illustrates that detergent extraction of extracellular parasites with 1% Triton X-100 in PBS removes the surface antigen P30/SAG1 (red) but the tagged RNG1 protein (green) continues to localize to an apical ring. Top row: unextracted samples; bottom row: extracted samples, displayed as merged phase-contrast/immunofluorescence, immunofluorescence and phase-contrast alone. (**b**) An immunoblot of the YFP-tagged RNG1 gene probed with an anti-GFP antibody identifies a band at the predicted size of ~36 kDa, and this antigen partitions to the detergent-insoluble parasite cytoskeleton. Samples: (1) total lysate from the RNG1-YFP line; (2) detergent-insoluble fraction; (3) detergent-soluble fraction (TCA precipitated); and (4) total lysate from wild-type RH strain *Toxoplasma* tachyzoites. (**c** and **d**) Deoxycholate extraction of tachyzoites frees the *Toxoplasma* subpellicular microtubules, APR and conoid to illuminate the relationship between these structures. Images in (c) are presented as merged red and green images (top) and with the tubulin staining alone (red, bottom). (c) Images 1–4 illustrate that the twenty-two subpellicular microtubules (red, anti-*Toxoplasma* tubulin antibody) radiate from a RNG1-YFP containing structure (green). A collapsed conoid is apparently present in Images 3 and 4 (arrows). The RNG1-YFP ring [(c) Images 5 and 6] viewed from the side illustrates that the label is located beneath the extended conoid (arrows) and above the subpellicular microtubules. Image 7 in (c) illustrates an extracted parasite where the conoid is either retracted or lost from the sample. (d) Images 1 and 2 are two examples of a disintegrating APR structure; the conoid is most visible in the tubulin alone images (arrows). RNG1-YFP is located at the minus ends of the separating microtubules in a small dot-like pattern. All scale bars = 2 μm.

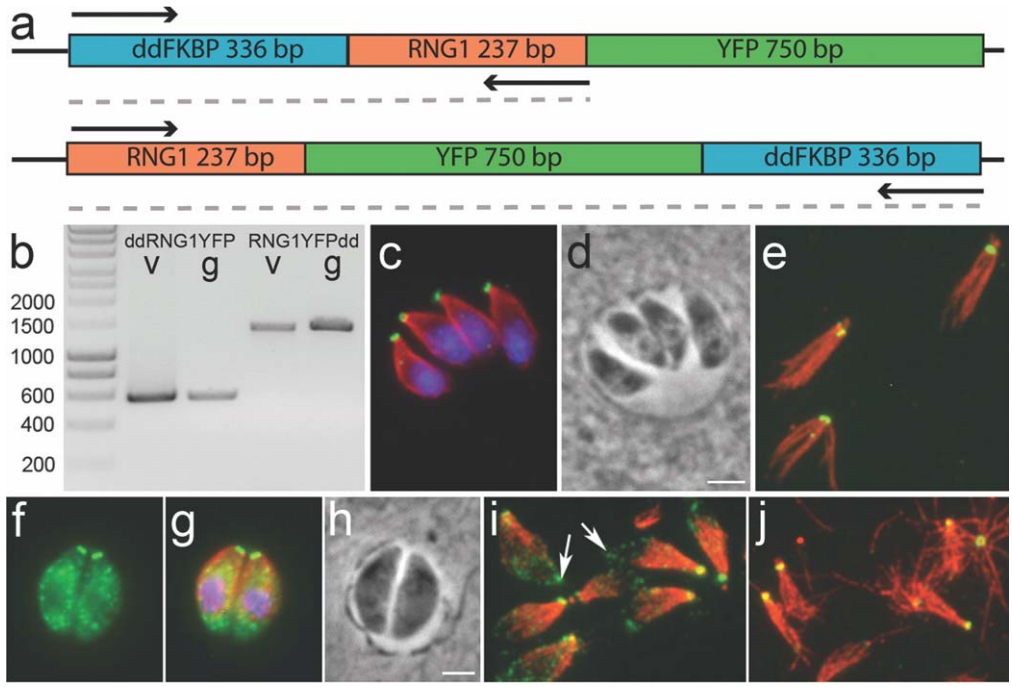

Fig. 6. Protein silencing and over-expression constructs for RNG1. (**a**) Illustrates the organization of two independent silencing constructs which place the ddFKBP domain at the amino (top) or carboxy (bottom) termini of RNG1-YFP constructs. (**b**) Image of an agarose gel with diagnostic amplification products from vector control (v) or genomic (g) DNA of the constructs in (a). Fluorescence microscopy (ddFKBP-RNG1-YFP in green and anti-tubulin staining in red) of parasites passed for 20 hours without Shield1 shows no diminution of signal in intracellular (**c,d**) or extracellular (**e**) parasites. Ectopic expression of RNG1-YFP causes parasites to have cytoplasmic aggregates of RNG1-YFP visible in intracellular (**f–h**) and extracellular parasites (**i**). When extracellular parasites are extracted with deoxycholate, only apical RNG1-YFP labeling is retained, other RNG1-YFP aggregates are lost (**j**).

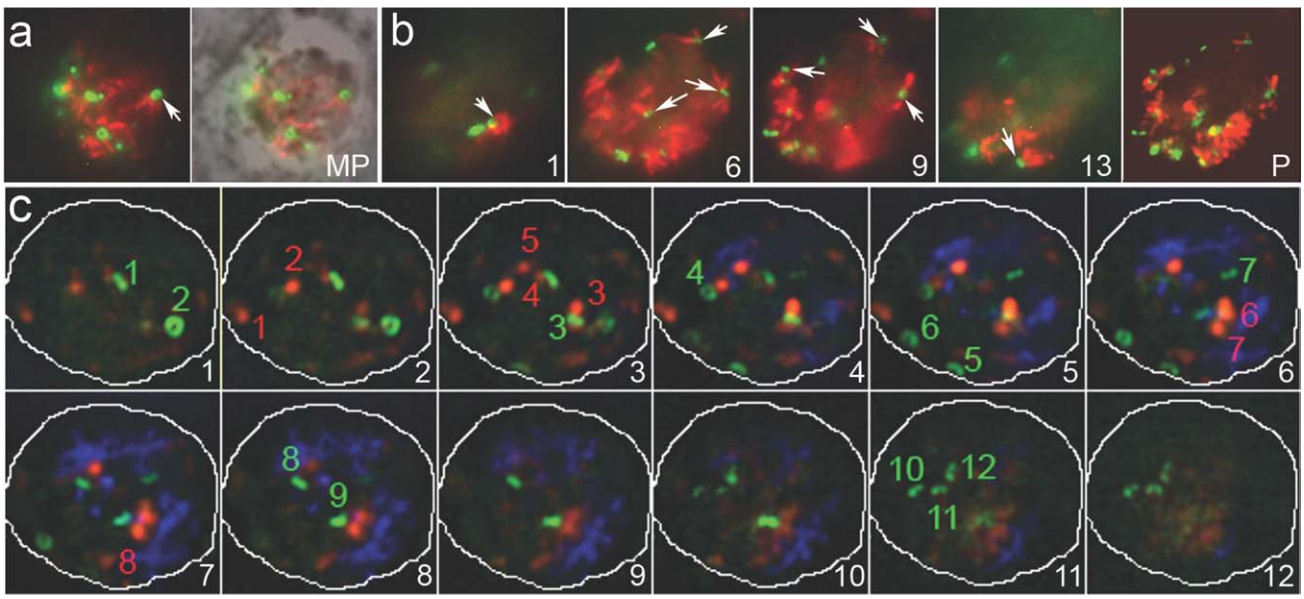

Fig. 7. Oryzalin-treated intracellular parasites continue to replicate RNG1-YFP-containing rings in the absence of microtubules, nuclear division and cytokinesis. RNG1-YFP parasites in HFF host cells treated for 24 hours with 2.5 μM oryzalin. (**a**) Immunofluorescence and fluorescence merged with phase-contrast (MP) of RNG1-YFP ring structures (green) which continue to form and in some cases appear to nucleate short microtubules (red). (**b**) Sections 1, 6, 9 and 13 from a deconvolved Z-series also shown as a complete projection (P) of an oryzalin-treated parasite with multiple RNG1-YFP rings (green) associated with short microtubules (red). (**c**) The number of rings (12) does not closely correlate with the number of duplicated centrioles (8), which also continue to replicate in an unchecked fashion in oryzalin-treated tachyzoites.

its cytosolic degradation by the proteasome. FRAP studies are typically used to evaluate rates of protein exchange, but would be extremely challenging to perform to analyze RNG1 integration kinetics: it is nearly impossible to find parasites in a stage where daughters have RNG1 labeling [such as in Fig. 2b (Image 3)]. This stage must be exceedingly transient: most parasites do not exhibit daughter labeling [Figs. 2b (Images 1 and 2)] or capture labeled daughters as they emerge from the mother (Fig. 2d).

Ectopic RNG1 Expression Does Not Alter Replication or Timing of Incorporation into the APR

In order to assess the effects of inappropriate expression of RNG1 on endodyogeny, we used expression of the RNG1 gene driven by the α1-tubulin promoter to express RNG1 throughout the cell cycle. We modified the established GRASP55-YFP construct [Hartmann et al., 2006] so that the GRASP55 gene was replaced by RNG1. This plasmid was transformed into RH strain parasites and stable transformants were selected in chloramphenicol. We observed a similar phenotype in both transient assays and stable isolated lines. Unregulated expression of RNG1-YFP did not lead to additional ring structures, alter normal replication or permit integration of RNG1 into the APR structure at an earlier point in the cell cycle. Extra RNG1-YFP protein is located in aggregate structures that are distributed throughout the cytoplasm (Figs. 6f–h). No additional changes in parasite morphology are observed. Unextracted extracellular parasites exhibit YFP-tagged protein aggregates, evident at the cell periphery (Fig. 6i, arrows). These punctate spots are extracted by deoxycholate treatment and so do not directly interact with the subpellicular microtubules. In contrast, the APR-associated RNG1 is retained in these samples (Fig. 6j).

RNG1 Structures Continue to Form when Nuclear Division and Cytokinesis are Inhibited

Treatment with 2.5 μM oryzalin blocks nuclear division and cytokinesis by inhibiting microtubule polymerization in intracellular parasites [Stokkermans et al., 1996; Shaw et al., 2000; Morrissette and Sibley, 2002b]. When RNG1-YFP parasites in HFF host cells are treated for 24–48 hours with oryzalin, RNG1-YFP ring structures continue to form (Fig. 7). In some cases, short microtubules re-polymerize and appear to be nucleated from the duplicated RNG1-YFP rings (Figs. 7a and 7b). The number of rings that form (12) is distinct from the number of duplicated centrioles (8), which also continue to replicate in an unchecked fashion in oryzalin treated cells (Fig. 7c). Since *Toxoplasma* replication by endodyogeny is nearly synchronous, we would predict both APR and centriole numbers to be factors of two. The observation of 8 centrioles is consistent with this expectation, but we would predict the corresponding number of rings to be 4, 8, or 16, plus one, to account for the original maternal ring which is not disassembled. It is possible that our ability to accurately count either centrioles or rings is compromised by their aggregation in oryzalin-treated parasites. Alternately, we may be observing accurate numbers, where duplication of these independent MTOCs is only modestly linked during replication, a conclusion that may be consistent with previous observations of the formation of extra daughter buds during endodyogeny [Hu, et al. 2002a].

Discussion

Eukaryotic organisms have devised diverse ways to organize and regulate microtubules through MTOCs [Pickett-Heaps, 1969; Graf et al., 2004; Wiese and Zheng, 2006; Luders and Stearns, 2007]. MTOCs include centrioles and centriole-containing centrosomes found in diverse organisms ranging from protozoa through vertebrates, the spindle-pole body structures of fungi and dispersed structures in higher land plants. Both fungi and higher land plants are thought to have lost the ability to form centrioles but retain some centriole components such as γ-tubulin and centrin. Apicomplexans exploit two distinct MTOCs: centrioles and the APR to independently organize the two discrete microtubule populations. Centrioles are found at the poles of the intranuclear spindle of *Toxoplasma* tachyzoites and are likely to play a role in chromosome segregation and spindle function. Markers of *Toxoplasma* centrioles include antibodies or fluorescent protein fusions to centrin-1 or SF-assemblin [Striepen et al., 2000; Morrissette and Sibley, 2002b; Lechtreck, 2003; Hu et al., 2006]. The APR organizes the subpellicular microtubules, which, as an early and essential component of daughter buds, are likely to play a role in cytokinesis. The APR is only found in apicomplexan organisms and previously characterized MTOC markers are not localized to this structure which nucleates a highly organized array of a set number of microtubules that extend for a fixed length [Nichols and Chiappino 1987; Russell and Burns 1984; Morrissette and Sibley 2002a]. Although it is an extremely late APR marker, as a constituent of this novel MTOC, RNG1 is a valuable tool to localize this structure and define its components.

Organisms classified as apicomplexans are named for a characteristic array of apical structures which facilitate invasion of host cells, including the rhoptries, micronemes, APR and conoid. Apicomplexans are grouped with the phyla Ciliophora (ciliates) and Dinophyceae (dinoflagellates) in the infrakingdom Alveolata, along with "enigmatic" organisms which have intermediate features and do not explicitly fall into a defined phylum [Leander and Keeling, 2003; Gould et al., 2008]. Some non-apicomplexan alveolates such as *Perkinsus* and *Colpodella* have conoid structures while many apicomplexans (such as *Plasmodium* spp.) do not. This suggests that the last common ancestor of all apicomplexans possessed a conoid, and the absence of this organelle in most apicomplexan lineages is due to a secondary loss of this structure.

Our data indicates that RNG1 is a component of the APR, an organelle which serves to organize subpellicular microtubules in apicomplexans. Although all apicomplexan organisms contain an APR, genome database searching only identified related RNG1 homologs in genomes for the closely related

parasites *Neospora caninum* and *Sarcocystis neurona*. As discussed above, this may be explained by the small size and low complexity of the RNG1 protein. There are certainly genes for proline-rich proteins in other apicomplexan genomes which may represent the orthologous protein in these organisms. However, it is also possible that RNG1 was lost from some lineages, perhaps in tandem with loss of the conoid. This latter possibility might imply that RNG1 serves to coordinate interactions between the APR and the conoid. It should also be noted that there are no obvious RNG1 homologs in available EST data from non-apicomplexan alveolates, as assessed by searching for sequences that encode similar proteins (J. Tran and N. Morrissette, unpublished observations).

Studies using diverse fluorescently tagged proteins have shown that *Toxoplasma* replication is a complex, ordered event [Striepen et al., 2000; Hu et al., 2002a; Gubbels et al., 2006, 2008; Ferguson et al., 2008; Gordon et al., 2008; Hu, 2008; Nishi et al., 2008]. We show here that RNG1 is a late component of the developing APR, appearing only after nuclear division is complete and daughter buds are quite mature. Recent array data validates these observations, as the RNG1 gene is profiled as having a mitotic/post-mitotic stage expression pattern which peaks at 3–4 hours after release from a thymidine kinase block (Michael White, University of South Florida, January 28, 2010, personal communication). Moreover, a recently identified AP-2-like transcription factor that is only expressed after nuclear division is likely to be a regulator of RNG1 expression (M. White, personal communication). When RNG1-YFP expression is driven by the α-tubulin promoter, producing RNG1-YFP throughout the cell cycle, excess protein aggregates in the cell cytoplasm. We do not observe premature incorporation of RNG1-YFP into the APR or formation of additional APR structures, indicating that late recruitment of RNG1 to the APR is not simply a function of tightly controlled transcription and translation.

Formation of two daughter APRs with associated subpellicular microtubules and sheets of IMC occurs in an early stage of endodyogeny. Collectively, these structures are required to enclose daughter organelles for inheritance. We show here that RNG1 appears on daughter parasites only after nuclear scission is complete. Since subpellicular microtubule nucleation from the APR clearly occurs prior to completion of division of the horseshoe shaped nucleus, RNG1 is dispensable for this process. The tightly regulated appearance of RNG1 after nuclear division and at the very conclusion of daughter cell formation may indicate that it regulates an aspect of daughter cell emergence. Maternal subpellicular microtubules, APR and IMC dissociate from the plasma membrane very late in endodyogeny. These structures are discarded in the residual body (c.f. Fig. 2d), and the two daughter parasites adopt the maternal plasma membrane which "zippers" over their IMC in concert with membrane scission events. Daughter buds cannot form when intracellular *Toxoplasma* tachyzoites are treated with 2.5 μM oryzalin, which disrupts all parasite microtubules and consequently inhibits the microtubule-driven processes of mitosis (chromosome segregation) and cytokinesis (daughter bud formation). Expression of RNG1 and its integration into duplicated APR structures occurs in the absence of microtubule function, suggesting that formation of the APR is independent of microtubule function but that in concert with microtubule function drives daughter cell formation.

Acknowledgments

We are grateful to Vern Carruthers (University of Michigan) who recognized that we would be interested in a *Toxoplasma* line that contained a tagged protein, which localized in an apical ring pattern and gave us this line prior to its first published description. Daniel Howe and Christopher Schardl (Advanced Genetic Technologies Center, University of Kentucky) kindly granted us access to "in progress" data for the *Sarcocystis neurona* genome project. Dan Goldberg (Washington University) provided us with a plasmid containing the FKBP12 destabilization domain for inclusion into our constructs. Peter Bradley (UCLA) and Jeff Salisbury (Mayo Clinic) kindly provided antibodies against ISP1 and centrin, respectively. We had important and interesting conversations concerning the *Toxoplasma* cell cycle, array data and AP-2 proteins with Michael White (University of South Florida). We thank Lawton Chung and David Wood for technical assistance. Research presented in this article was supported by NIH grant AI067981 to NSM.

References

Beck JR, Rodriguez-Fernandez IA, de Leon JC, Huynh MH, Carruthers VB, Morrissette NS, Bradley PJ 2010. A novel family of Toxoplasma IMC proteins display a hierarchical organization and function in coordinating parasite division. PLoS Pathogens: in press.

Black MW, Boothroyd JC. 2000. Lytic cycle of Toxoplasma gondii. Microbiol Mol Biol Rev 64:607–623.

Burg JL, Perelman D, Kasper LH, Ware PL, Boothroyd JC. 1988. Molecular analysis of the gene encoding the major surface antigen of Toxoplasma gondii. J Immunol 141:3584–3591.

Cohen AM, Rumpel K, Coombs GH, Wastling JM. 2002. Characterisation of global protein expression by two-dimensional electrophoresis and mass spectrometry: proteomics of Toxoplasma gondii. Int J Parasitol 32:39–51.

Del Carmen MG, Mondragon M, Gonzalez S, Mondragon R. 2009. Induction and regulation of conoid extrusion in Toxoplasma gondii. Cell Microbiol 11:967–982.

Dobrowolski J, Sibley LD. 1997. The role of the cytoskeleton in host cell invasion by Toxoplasma gondii. Behring Inst Mitt (99):90–6.

Ferguson DJ, Sahoo N, Pinches RA, Bumstead JM, Tomley FM, Gubbels MJ. 2008. MORN1 has a conserved role in asexual and sexual development across the apicomplexa. Eukaryot Cell 7:698–711.

Gaskins E, Gilk S, DeVore N, Mann T, Ward G, Beckers C. 2004. Identification of the membrane receptor of a class XIV myosin in Toxoplasma gondii. J Cell Biol 165:383–393.

Gilbert LA, Ravindran S, Turetzky JM, Boothroyd JC, Bradley PJ. 2007. Toxoplasma gondii targets a protein phosphatase 2C to the nuclei of infected host cells. Eukaryot Cell 6:73–83.

Gilk SD, Raviv Y, Hu K, Murray JM, Beckers CJ, Ward GE. 2006. Identification of PhIL1, a novel cytoskeletal protein of the Toxoplasma gondii pellicle, through photosensitized labeling with 5-[125I]iodonaphthalene-1-azide. Eukaryot Cell 5:1622–1634.

Gish W, States DJ. 1993. Identification of protein coding regions by database similarity search. Nat Genet 3:266–272.

Gordon JL, Beatty WL, Sibley LD. 2008. A novel actin-related protein is associated with daughter cell formation in Toxoplasma gondii. Eukaryot Cell 7:1500–1512.

Gould SB, Tham WH, Cowman AF, McFadden GI, Waller RF. 2008. Alveolins, a new family of cortical proteins that define the protist infrakingdom Alveolata. Mol Biol Evol 25:1219–1230.

Graf R, Daunderer C, Schulz I. 2004. Molecular and functional analysis of the dictyostelium centrosome. Int Rev Cytol 241:155–202.

Gubbels MJ, Vaishnava S, Boot N, Dubremetz JF, Striepen B. 2006. A MORN-repeat protein is a dynamic component of the Toxoplasma gondii cell division apparatus. J Cell Sci 119:2236–2245.

Gubbels MJ, White M, Szatanek T. 2008. The cell cycle and Toxoplasma gondii cell division: tightly knit or loosely stitched? Int J Parasitol 38: 1343–1358.

Hartmann J, Hu K, He CY, Pelletier L, Roos DS, Warren G. 2006. Golgi and centrosome cycles in Toxoplasma gondii. Mol Biochem Parasitol 145: 125–127.

Heintzelman MB, Schwartzman JD. 1997. A novel class of unconventional myosins from Toxoplasma gondii. J Mol Biol 271:139–146.

Hepler PK, Huff CG, Sprinz H. 1966. The fine structure of the exoerythrocytic stages of Plasmodium fallax. J Cell Biol 30:333–358.

Herm-Gotz A, Weiss S, Stratmann R, Fujita-Becker S, Ruff C, Meyhofer E, Soldati T, Manstein DJ, Geeves MA, Soldati D. 2002. Toxoplasma gondii myosin A and its light chain: a fast, single-headed, plus-end-directed motor. EMBO J 21:2149–2158.

Herm-Gotz A, Delbac F, Weiss S, Nyitrai M, Stratmann R, Tomavo S, Sibley LD, Geeves MA, Soldati D. 2006. Functional and biophysical analyses of the class XIV Toxoplasma gondii myosin D. J Muscle Res Cell Motil 27: 139–151.

Herm-Gotz A, Agop-Nersesian C, Munter S, Grimley JS, Wandless TJ, Frischknecht F, Meissner M. 2007. Rapid control of protein level in the apicomplexan Toxoplasma gondii. Nat Methods 4:1003–1005.

Hettmann C, Herm A, Geiter A, Frank B, Schwarz E, Soldati T, Soldati D. 2000. A dibasic motif in the tail of a class XIV apicomplexan myosin is an essential determinant of plasma membrane localization. Mol Biol Cell 11: 1385–1400.

Higgins DG, Thompson JD, Gibson TJ. 1996. Using CLUSTAL for multiple sequence alignments. Methods Enzymol 266:383–402.

Hu K. 2008. Organizational changes of the daughter basal complex during the parasite replication of Toxoplasma gondii. PLoS Pathog 4:e10.

Hu K, Mann T, Striepen B, Beckers CJ, Roos DS, Murray JM. 2002a. Daughter cell assembly in the protozoan parasite Toxoplasma gondii. Mol Biol Cell 13:593–606.

Hu K, Roos DS, Murray JM. 2002b. A novel polymer of tubulin forms the conoid of Toxoplasma gondii. J Cell Biol 156:1039–1050.

Hu K, Johnson J, Florens L, Fraunholz M, Suravajjala S, DiLullo C, Yates J, Roos DS, Murray JM. 2006. Cytoskeletal components of an invasion machine--the apical complex of Toxoplasma gondii. PLoS Pathog 2:e13.

Huynh MH, Carruthers VB. 2009. Tagging of endogenous genes in a Toxoplasma gondii strain lacking Ku80. Eukaryot Cell 8:530–539.

Karasov AO, Boothroyd JC, Arrizabalaga G. 2005. Identification and disruption of a rhoptry-localized homologue of sodium hydrogen exchangers in Toxoplasma gondii. Int J Parasitol 35:285–291.

Leander BS, Keeling PJ. 2003. Morphostasis in alveolate evolution. Trends Ecol Evol 18:395–402.

Lechtreck KF. 2003. Striated fiber assemblin in apicomplexan parasites. Mol Biochem Parasitol 128:95–99.

Levene ND. 1988. The protozoan phylum Apicomplexa. Boca Raton, FL: CRC Press; ISBN-10:0849346533.

Luders J, Stearns T. 2007. Microtubule-organizing centres: a re-evaluation. Nat Rev Mol Cell Biol 8:161–167.

Mann T, Beckers C. 2001. Characterization of the subpellicular network, a filamentous membrane skeletal component in the parasite Toxoplasma gondii. Mol Biochem Parasitol 115:257–268.

Mann T, Gaskins E, Beckers C. 2002. Proteolytic processing of TgIMC1 during maturation of the membrane skeleton of Toxoplasma gondii. J Biol Chem 277:41240–41246.

Mondragon R, Frixione E. 1996. Ca(2+)-dependence of conoid extrusion in Toxoplasma gondii tachyzoites. J Eukaryot Microbiol 43:120–127.

Monteiro VG, de Melo EJ, Attias M, de Souza W. 2001. Morphological changes during conoid extrusion in Toxoplasma gondii tachyzoites treated with calcium ionophore. J Struct Biol 136:181–189.

Morrissette NS, Sibley LD. 2002a. Cytoskeleton of apicomplexan parasites. Microbiol Mol Biol Rev 66:21–38.

Morrissette NS, Sibley LD. 2002b. Disruption of microtubules uncouples budding and nuclear division in Toxoplasma gondii. J Cell Sci 115: 1017–1025.

Morrissette NS, Murray JM, Roos DS. 1997. Subpellicular microtubules associate with an intramembranous particle lattice in the protozoan parasite Toxoplasma gondii. J Cell Sci 110:35–42.

Nichols BA, Chiappino ML. 1987. Cytoskeleton of Toxoplasma gondii. J Protozool 34:217–226.

Nishi M, Hu K, Murray JM, Roos DS. 2008. Organellar dynamics during the cell cycle of Toxoplasma gondii. J Cell Sci 121:1559–1568.

Pelletier L, Stern CA, Pypaert M, Sheff D, Ngo HM, Roper N, He CY, Hu K, Toomre D, Coppens I and others. 2002. Golgi biogenesis in Toxoplasma gondii. Nature 418:548–552.

Pezzella N, Bouchot A, Bonhomme A, Pingret L, Klein C, Burlet H, Balossier G, Bonhomme P, Pinon JM. 1997. Involvement of calcium and calmodulin in Toxoplasma gondii tachyzoite invasion. Eur J Cell Biol 74: 92–101.

Pickett-Heaps JD. 1969. The evolution of the mitotic apparatus: an attempt at comparative ultrastructural cytology in dividing plant cells. Cytobios 1: 257–280.

Radke JR, Striepen B, Guerini MN, Jerome ME, Roos DS, White MW. 2001. Defining the cell cycle for the tachyzoite stage of Toxoplasma gondii. Mol Biochem Parasitol 115:165–175.

Read M, Sherwin T, Holloway SP, Gull K, Hyde JE. 1993. Microtubular organization visualized by immunofluorescence microscopy during erythrocytic schizogony in Plasmodium falciparum and investigation of post-translational modifications of parasite tubulin. Parasitology 106:223–232.

Roos DS, Donald RG, Morrissette NS, Moulton AL. 1994. Molecular tools for genetic dissection of the protozoan parasite Toxoplasma gondii. Methods Cell Biol 45:27–63.

Russell DG, Burns RG. 1984. The polar ring of coccidian sporozoites: a unique microtubule-organizing centre. J Cell Sci 65:193–207.

Shaw MK, Compton HL, Roos DS, Tilney LG. 2000. Microtubules, but not actin filaments, drive daughter cell budding and cell division in Toxoplasma gondii. J Cell Sci 113:1241–1254.

Soldati D, Meissner M. 2004. Toxoplasma as a novel system for motility. Curr Opin Cell Biol 16:32–40.

States DJ, Gish W. 1994. Combined use of sequence similarity and codon bias for coding region identification. J Comput Biol 1:39–50.

Stedman TT, Sussmann AR, Joiner KA. 2003. Toxoplasma gondii Rab6 mediates a retrograde pathway for sorting of constitutively secreted proteins to the Golgi complex. J Biol Chem 278:5433–5443.

Stokkermans TJ, Schwartzman JD, Keenan K, Morrissette NS, Tilney LG, Roos DS. 1996. Inhibition of Toxoplasma gondii replication by dinitroaniline herbicides. Exp Parasitol 84:355–370.

Striepen B, Crawford MJ, Shaw MK, Tilney LG, Seeber F, Roos DS. 2000. The plastid of Toxoplasma gondii is divided by association with the centrosomes. J Cell Biol 151:1423–1434.

Swedlow JR, Hu K, Andrews PD, Roos DS, Murray JM. 2002. Measuring tubulin content in Toxoplasma gondii: a comparison of laser-scanning confocal and wide-field fluorescence microscopy. Proc Natl Acad Sci USA 99: 2014–2019.

Wiese C, Zheng Y. 2006. Microtubule nucleation: gamma-tubulin and beyond. J Cell Sci 119:4143–4153.